NEW APPROACHES IN THE SEISMOTECTONICS OF THE MARGINAL DACIDES UNIT

Raluca DINESCU[1,2], Ioan MUNTEANU[3], Eugen OROS[1], Mihaela POPA[4], Mircea RADULIAN[1,4,5], Andreea CHIRCEA[1,6]

[1]National Institute for Earth Physics, 12 Calugareni Street, 077125 Magurele, Romania
[2]University of Bucharest, Doctoral School of Geology, 6 Traian Vuia Street, 020956 Bucharest, Romania
[3]University of Bucharest, Faculty of Geology and Geophysics, 1 N. Balcescu Blv., 010041, Bucharest, Romania
[4]Academy of Romanian Scientists, 3 Ilfov Street, 030167 Bucharest, Romania
[5]Romanian Academy, 125 Calea Victoriei, 010071 Bucharest, Romania
[6]University of Bucharest, Faculty of Physics, 405 Atomistilor Street, 077125 Magurele, Romania
e-mail: raluca.dinescu@infp.ro

DOI: 10.5281/zenodo.14228918

Abstract. The goal of this study is to perform a cross-correlation analysis of the earthquake sequences, recorded between 2014 and 2016 in the Caransebeș-Mehadia Area (CMA), in Romania, and to correlate the results with the surface geology, for a better understanding of the neotectonics processes taking place in the South-Western Carpathian Bend Zone. The apparent sparse seismicity between 1886 and 2005 in CMA is mostly due to the lack of seismic stations in the region before 2006. The image changed with 2006, when the recorded event rate increased to 3-15 events/year between 2006-2013 and 2017-2023 and to 45-70 events/year between 2014–2016-time intervals. The high number of events recorded between 2014 and 2016 is related to the occurrence of the three seismic sequences in the CMA: between 31/10/2014 and 20/02/2015, between 23/11/2015 and 28/12/2015 and between 27/07/2016 and 29/08/016. We apply the cross correlation analysis technique for the events recorded in the 2014-2016 time period to identify events belonging to a cluster and to identify new events undetected by routine seismic analysis. The templates used for the analysis were selected from the events recorded in ROMPLUS. We consider an event as belonging to a cluster if the cross-correlation coefficient is equal to or greater than 0.7. Four templates were used and the results show a detection of 37 new events belonging to the seismic sequences from CMA. The distribution of the epicentres shows a migration from west to east suggesting a possible post-triggering effect after the 2014 mainshock.

Key words: Caransebeș-Mehadia Area, seismic swarm, cross-correlation

1. INTRODUCTION

The evolution of the Alpine orogenic system is a continuous and ongoing tectonic process that started in Cretaceous times, shaping the mountain chains from the Alps to the Caucasus and further eastward including the Himalayas, with the Romanian Carpathians as one the most seismically active sectors of this system. The intermediate-depth earthquakes from the Vrancea source and crustal seismicity spread along the South-Eastern Carpathians Bend Zone (SECBZ; Fig. 1a) at the contact between orogen and platform areas are evident proofs of the active deformation process affecting the Carpathian Arc sector (Popa *et al.*, 2018).

The seismicity as well as the deformation does not restrain to this sector and extends to the west along the Southern Carpathians (Fig. 1a) through the Făgăraș-Câmpulung Region and further in the South-Western Carpathian Bend Zone (SWCBZ).

Continuous deformation in the SWCBZ region is outlined by the crustal seismicity concentrated along the faults system bordering the Neogene intramountain basins, like Caransebeș-Mehadia (CMB), Hațeg (HB), Petroșani (PB), Bozovici (BB) and Orșova (OB) basins highlighted in figures 1b and 1c. Associated with this deformation, several seismic sequences have been recorded during the last decade with

the help of modern equipment's, which allow better event localization and definition, and determination of focal mechanism, an important parameter for the understanding of the present day stress regimes and hence the neotectonic processes.

We consider the region from the Olt River to the Danube River, along the Carpathian Orogen as the SWCBZ (Fig. 1a). The SWCBZ is affected by crustal seismicity (Fig. 1b, Fig. 2) and seismic sequences concentrated in the Neogene intramountain basins, such as CMB, HB, PB and OB (Figs. 3a and 3b). Our study is related to the CMB and nearby regions, named as Caransebeș-Mehadia Area (CMA).

A relative intensification of seismicity in the CMA area was recorded between 2014 and 2016 (Fig. 4a) providing the best quality data we have available until now. Three seismic sequences occurred during this time interval. The first sequence started on 31/10/2014 with a main shock of magnitude Mw = 4.1 followed by 86 aftershocks in the ROMPLUS catalogue (Oncescu et al, 1999, updated; Popa *et al.*, 2022). Two other clusters of swarm type were recorded from 23/11/2015 to 28/12/2015 (10 events, with a magnitude between 1.5 and 1.9 in ROMPLUS) and from 27/07/2016 to 29/08/2016 (41 events, with a magnitude between 1.2 and 2.5 in ROMPLUS). The sequences from 2014 to February 2015 were studied by Placintă *et al.* (2016) and Popa *et al.* (2018).

The goal of this study is to perform an exhaustive analysis of the data related to these sequences and to investigate how they correlate with the geological structure, main basin faults, and seismicity in the CMA area. Finally, we outline the contribution of the new instrumental data to our understanding of the neotectonics of the CMA area.

2. GEOLOGICAL FRAMEWORK

The Carpathian Orogen, part of the Alpine system, has been structured since mid-Cretaceous with the inversion of the former Mesozoic rift system and was gradually shaped in the present-day geometry by the latest Cenozoic deformation, with the formation of the Carpathian fold and thrust belt (Moldavides) coeval with the opening of the Pannonian Basin (Maţenco and Radivojevic, 2012). The highly arcuate geometry of the Carpathian Mountains is a consequence of the continental slab rollback common with some other orogens from the Mediterranean area (Maţenco and Radivojevic, 2012). The Romanian Carpathians stretching from one bend to another, include the most active tectonic zone in the entire Alpine system, the East Carpathians Bend zone, with the Vrancea seismic zone recording a large number of earthquakes (Popescu and Radulian, 2001). The Southern Carpathians are part of the Dacia mega-unit, an important part of the European continent (Schmid *et al.*, 2008). The Dacia block departed from the continent during Middle-Late Jurassic times and gradually joined back during Cretaceous-Miocene times, while the Ceahlău-Severin Nappe and easterly oceanic to thinned continental remnant oceans closed (Săndulescu, 1988; Maţenco and Radivojevic, 2012).

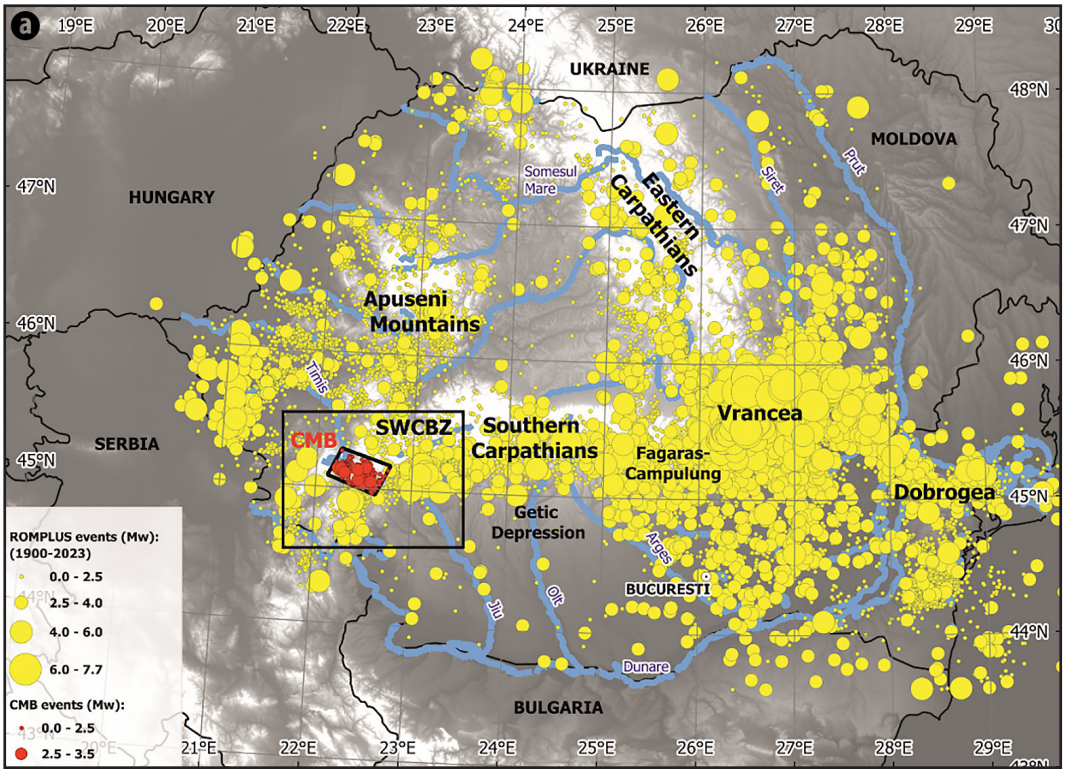

Fig. 1. (**a**) The distribution of the events from ROMPLUS catalogue (yellow dots) separated by magnitude intervals. The CMA region is highlighted with black square and red dots.

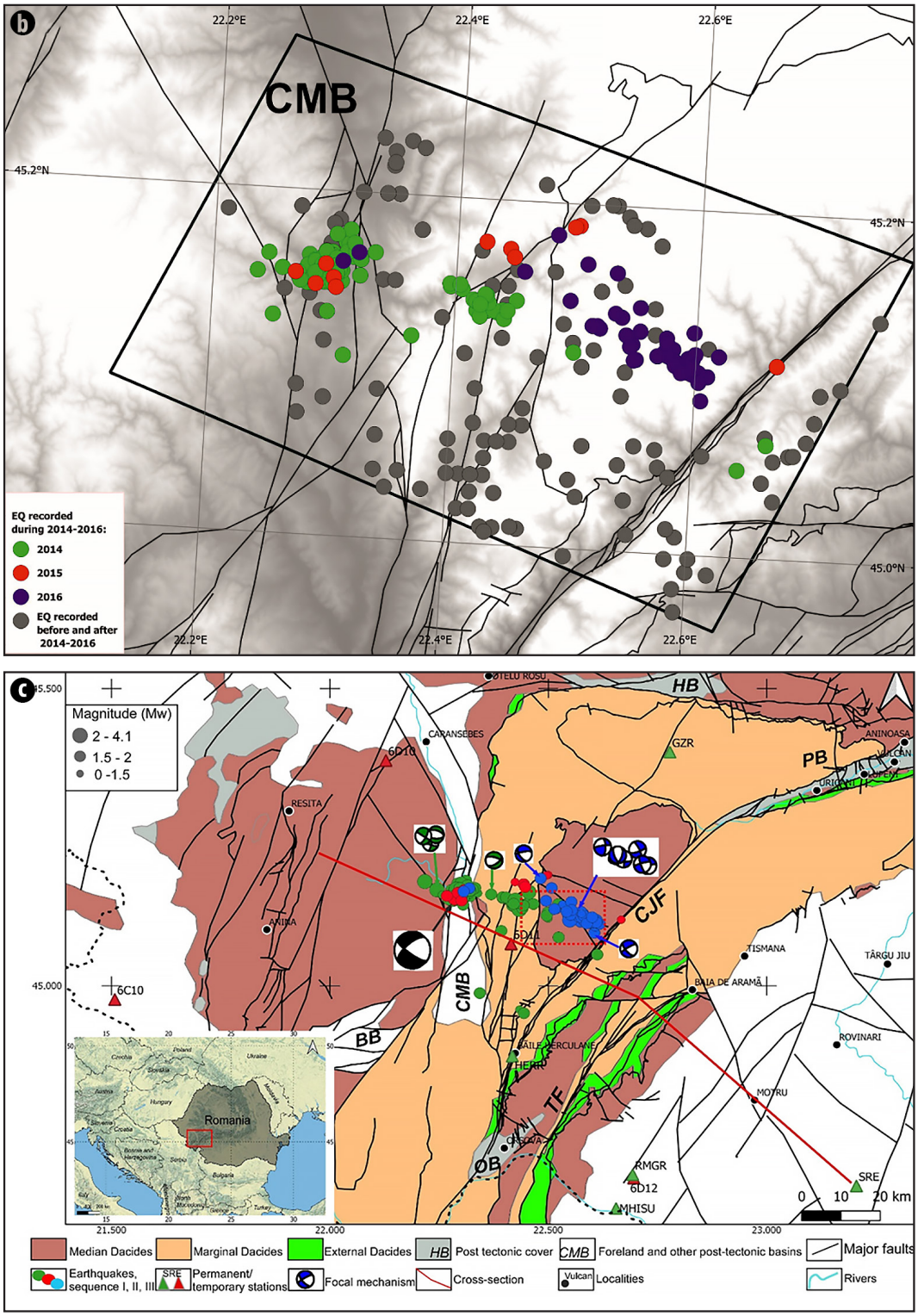

Fig. 1. (**b**) The distribution of the seismic events from the 2014-2016 sequences separated by year (2014 - green dots; 2015 - pink dots, 2015 - blue dots) and the events recorded before and after the 2014-2016 interval (grey dots). (**c**) Geological map of study zone (after Săndulescu *et al.*, 1978). The events of the seismic sections are represented by dots: I (green), II (red), III (blue). **CMB** – Caransebeș-Mehadia Basin, **HB** – Hațeg Basin, **PB** – Petroșani Basin, **OB** – Orșova Basin, **BB** – Bozovici Basin. Permanent seismic stations: **GZR** – Gura Zlata, **MHISU** – ISU Mehedinți, **RMGR** – Halanga-Turnu Severin, **SRE** – Strehaia. Temporary seismic stations: 6C10, 6D10, 6D11, 6D12. Fault lines: **CJF** – Cerna-Jiu Fault, **TF** – Timok Fault. The red line represents the transect in figure 2 (the cross-section through the SWCBZ after Ştefănescu *et al.*, 1988). Fault plane solutions (beachballs, BB) for the events from 2014-2015 (Popa *et al.*, 2018) and 2016 (10 events as part of this study) are indicated on the map – sequences: 1 (green BB), 3 (blue BB). Black BB (Mw = 4.1) for the 31/10/2014 event, reprocessed during this study.

The South Carpathians are affected by a large number of deformations with dextral strike-slip orientation followed by the clockwise rotation with NE movement of the Carpathian Orogen around the western corner of the Moesian Platform (Bala, 1997; Linzer *et al.*, 1998; Placintă *et al.*, 2016; Ghiță *et al.*, 2020).

The sedimentary CMA, located in the external part of the South Carpathians, has developed over the Median and Marginal Dacides basement nappes (Săndulescu, 1984), its evolution being related to the North-ward tectonic transport of the Carpathian Orogen during Paleogene-Quaternary times into current position (Popa *et al.*, 2018). The tectonic transport took place on deep crustal-scale faults, describing a general right lateral strike-slip system formed between the Moesian Platform and Carpathian Orogen (Maţenco *et al.*, 2007 and references therein). The gradual East-ward rotation accompanying the tectonic transport resulted in the stress field reorientation and deformation localization across numerous faults, either normal or reverse, associated with the main strike-slip movements (Fig. 1c). Associated with these faults are the sedimentary basins, which in numerous cases have been subsequently inverted or re-deformed and separated into sub-basins like the CMB (Fig. 1c and Fig. 2).

3. REGIONAL SEISMICITY IN THE SOUTH-WESTERN CARPATHIAN BEND ZONE

The seismic activity in the south-western part of Romania (Banat region and Danubian region) is related to different earthquake-prone clusters indicated in figure 3a: (1) Sânnicolau-Arad, (2) Timișoara and Banloc-Voiteg, (3) Oravița - Moldova-Nouă and Mehadia - Orșova, (4) Poiana Ruscă Mts. - Haţeg Basin - Bistra Valley (Fig. 3a), Gorj and Târgu-Jiu (Fig. 3b) in connection with specific regional geotectonic units (Radulian *et al.*, 2014; Oros and Diaconescu, 2015; Popa *et al.*, 2018; Ghiță *et al.*, 2020).

The last two, (3) and (4), clusters belonging to the western sector of the SWCBZ are characterized by a combination of sporadic and isolated events with clusters of earthquake sequences and swarms, located in the upper crust, down to 30 km depth.

The earthquakes are generated along the contact zone between the Carpathian Orogen and Getic Depression, mainly along the important faults such as the Cerna-Jiu Fault (CJF) and Neogene Intra-Carpathian basins: HB, CMB, PB and in the Târgu-Jiu Basin (TJB) to the east (Radulian *et al.*, 2014). According to ROMPLUS, more than 6000 events were recorded between 1639 and June 2023 in the western part of Southern Carpathians and among them only 410 events with a magnitude Mw greater than 2.5 (Figs. 3a and 3b). The strongest earthquakes recorded in this region of magnitude Mw = 5.6 were generated between the tectonic blocks of the Median Dacides, one in 1832 at the eastern edge (the contact with the Făgăraș-Câmpulung seismogenic zone), on the western part of Olt River, and the other in 1991, west to the Herculane seismic station (HERR), along the CJF (Berza and Drăgănescu, 1988; Oncescu *et al.*, 1999-updated).

The first important seismic cluster in the SWCBZ was recorded during the 1879-1880-time interval along the OF, close to Danube River (near Moldova Nouă city) (Fig. 3b). According to the ROMPLUS, the earthquake sequence started on 28/09/1879 (Oros, 2004) with two strong shocks, on 10/10/1879 (Mw = 5.3) and on 11/10/1879 (Mw = 5.3), followed by associated aftershocks that were recorded for almost seven months (13 events recorded in ROMPLUS). The seismic activity in this region during the 20th century was characterized by spatial clusters on the OF and CJF (Fig. 1c). A significant earthquake was recorded on 11/10/1910 (Mw = 4.3, according to Oncescu et al, 1999 or Mw = 5.3, according to Oros, 2011). The largest earthquake from the SWCBZ occurred on 18/07/1991, Mw = 5.6, I0 = 7,5 EMS (Oncescu et al, 1999, Oros *et al.*, 2008), along the CJF, nearby Herculane city, Herculane Spa-Mehadia area (Fig. 1c).

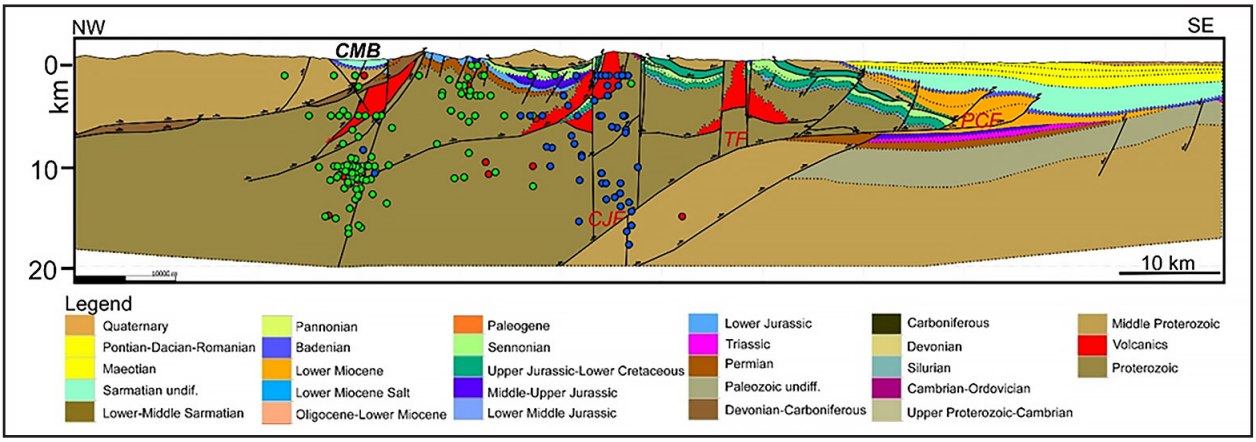

Fig. 2. Cross-section through the South Western Carpathians region (modified after Ştefănescu *et al.*, 1988, Popa *et al.*, 2018) – represented by the red line in figure 1c. The hypocentres projected on the cross-section are shown as dots (the same colours as in figures 1b and 1c). **CMB** – Caransebeș-Mehadia Basin; **CJF** – Cerna-Jiu Fault; **TF** – Târgu-Jiu Fault; **PCF** – Pericarpathian Fault.

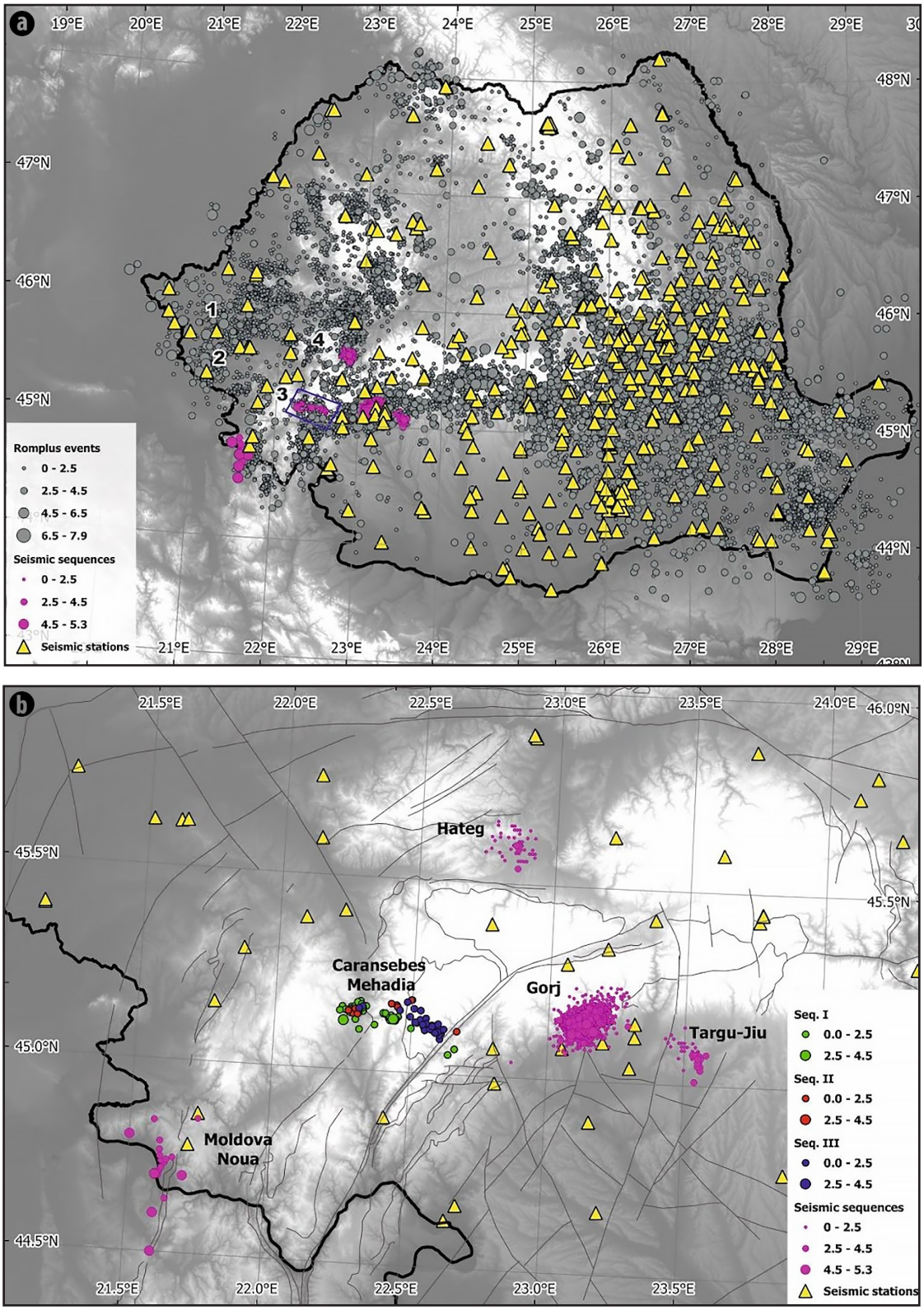

Fig. 3. (**a**) Seismic representation of the CMB (light blue dots inside dark blue polygon) events highlighted over the ROMPLUS events (grey dots) between 984 and 2023 with Mw-related symbol size. The pink dots represent the seismic and swarm sequences from SWCBZ between 1889 and 2016 (Oros, 2004; Radulian et al, 2014; Placinta et al, 2016; Popa et al, 2018 and this study). Earthquake prone-clusters: (1) Sânnicolau - Arad, (2) Timișoara and Banloc-Voiteg, (3) Oravița - Moldova-Nouă and Mehadia - Orșova, (4) Poiana Ruscă Mts - Haţeg Basin - Bistra Valley; Red polygon represents the zoom of figure 3b. (**b**) Sequences in the SWCBZ area: sequences 1 (green), 2 (red) and 3 (blue) in CMB and other sequences (pink). Symbol size scales with magnitude for three intervals: 0 - 2.5, 2.5 - 4.5, 4.5 - 5.5.

The Moldova Noua Region was affected again between 01/04/2002 and 31/08/2002 by a seismic sequence of 70 recorded events with magnitudes (Mw) between 2.0 and 3.6 (Oros, 2004; Popa *et al.*, 2018). Two sequences generated in 2011 in the HB, a swarm of 19 events recorded between 17/03/2011and 31/05/2011 and a sequence of 36 events (Mw = 2.0 - 4.0) recorded between 08/09/2011 and 31/10/2011 were investigated by Placintă *et al.* (2016) and Popa *et al.* (2018). Another cluster of seismicity is located at the eastern edge of our study region, in the Târgu-Jiu Basin, where an event with high magnitude (Mw = 5.2) was recorded in 1943 and a sequence of 40 events, identified and located nearby Târgu-Jiu – Târgu-Cărbunești, started in 30/12/2011 and lasted until 05/01/2012 (Radulian *et al.*, 2014). The seismic sequence from 2023, started on the 13th of February with a double-shock of 4.8 and 5.4 (Mw) followed by more than 4000 aftershocks with magnitudes between 1.1 and 4.6 (ROMPLUS).

4. SEISMICITY OF THE CARANSEBES-MEHADIA BASIN BETWEEN 1886 AND 2019

The CMA (highlighted by the pink dots inside the blue rectangle in figure 3a), located in the region called Danubian Seismic Zone (Radulian *et al.* 2000; Oros, 2007), was characterized by rare seismicity from 1886 to the present day. Since 1886 there were recorded in the ROMPLUS catalogue only 290 events, with 3 events recorded before 2006, 2 events in 1886 and 1 event in 1995, and the magnitudes (Mw) of these events being considered between 2 and 3 and with depths smaller than 15 km. Certainly, the small number of seismic stations operating in the SWCBZ for the 1886 – 2005 time period accounts for the small number of seismic events recorded in ROMPLUS. After 2006, 8 new seismic stations were installed in the region, and since then the rate of recorded event increased to about 3-15 earthquakes/year for the 2006-2013 time-interval and for the 2017-2023 time-interval (Fig. 4); for the 2014-2016-time interval the increase of recorded events up to 45-70 events/year and this increment is related to the occurrence of three seismic episodes in the CMA, along the Cerna-Jiu Fault System:

- Sequence I: 31/10/ 2014 – 20/02/2015 – the events that were reported over this time span can be separated into two groups (*Ia*) and (*Ib*)
- Sequence II: 23/11/2015 – 28/12/2015
- Sequence III: 27/07/2016 - 29/08/2016

The sequence I initiated with a high magnitude mainshock (Mw = 4.1, ML = 4.7), proceeded by 86 aftershocks identified and recorded in ROMPLUS catalogue. The mainshock seismic event that occurred on 31/10/2014 was the largest earthquake recently recorded in CMA. We considered the aftershock activity as being separated into two sub-sequences: sequence *Ia*, from 31/10/2014 to 15/12/2014 and sequence *Ib* from 15/12/2014 to 05/03/2015. Sequence *II* initiated on 23/11/2015 and lasted until 28/12/2015, and sequence *III*, recorded from 27/07/2016 until 29/08/2016 were considered to be both of swarm type with 10 events, and 41 events, respectively, as identified and recorded in ROMPLUS.

The behaviour of the sequence I is characterized by a rapid and effective energy release from the start considering the aftershock activity of small magnitude (Mw < 2.5) events in comparison with the magnitude of the mainshock (Mw 4.1). Also note the extended time duration for the aftershock low-scale recovery processes (one and a half months for sequence *Ia*, the first step, and three months for sequence *Ib*, the second stage). The sequence II, recorded between 23/11/2015 and 28/12/2015, consisted of only 10 recorded events in ROMPLUS, and it is located eastward from the first sequence. Sequence III shows the same eastward migration behaviour as the sequence II.

The epicentres configuration for the sequences I, II and III, represented in figure 4a, illustrates these two noticeable characteristics: a W-E extension and a migration in space and time from west to east: sub-sequence Ia located in the western side and sub-sequence Ib slightly prolongated to the right-east (shifted by about 10 km to the east) – sequence II more widely distributed in space partially overlaps the first and third sequences – sequence III is located in the eastern side.

The events of sequence I were recorded over a broad range of depths, between 1 and 33 km and moment-magnitudes (Mw) between 1.3 and 4.1 (ML= 0.5 - 4.7), while the seismic events of the sequence II and sequence III were located at depths smaller than 16.5 km. For the last two sequences there were recorded small-size seismic, with magnitudes (Mw) between 1.5 and 1.9, and between 1.2 and 2.5, respectively.

Previously analyses of the subsequence *Ia* were carried out by Placinta *et al.* (2016) and Popa *et al.* (2018). In this paper, we will include the analysis of the other sequences and include the results to outline how the seismicity features interact with the geotectonic setting of the SWCBZ.

5. CLUSTERING ANALYSIS

The earthquakes considered in this paper are located in the CMA and recorded in the ROMPLUS catalogue using the routine monitoring procedure. The RMS ranges from 0.03 to 0.86, the GAP from 38 to 202, and the number of stations used in the locating process varies from 3 to 62. First, we relocated with Antelope analysis software the events recorded in the CMA during the 2014–2016-time interval with greater location errors, such as depth errors and semi-axes errors. Then, to outline the clustering properties of the events in the CMA, we conducted cross-correlation analysis on the waveforms recorded starting with the main event from 31/10/2014 until the end of 2016. The results obtained for cluster III are more conclusive for the period 27/07/2016 – 29/08/2016.

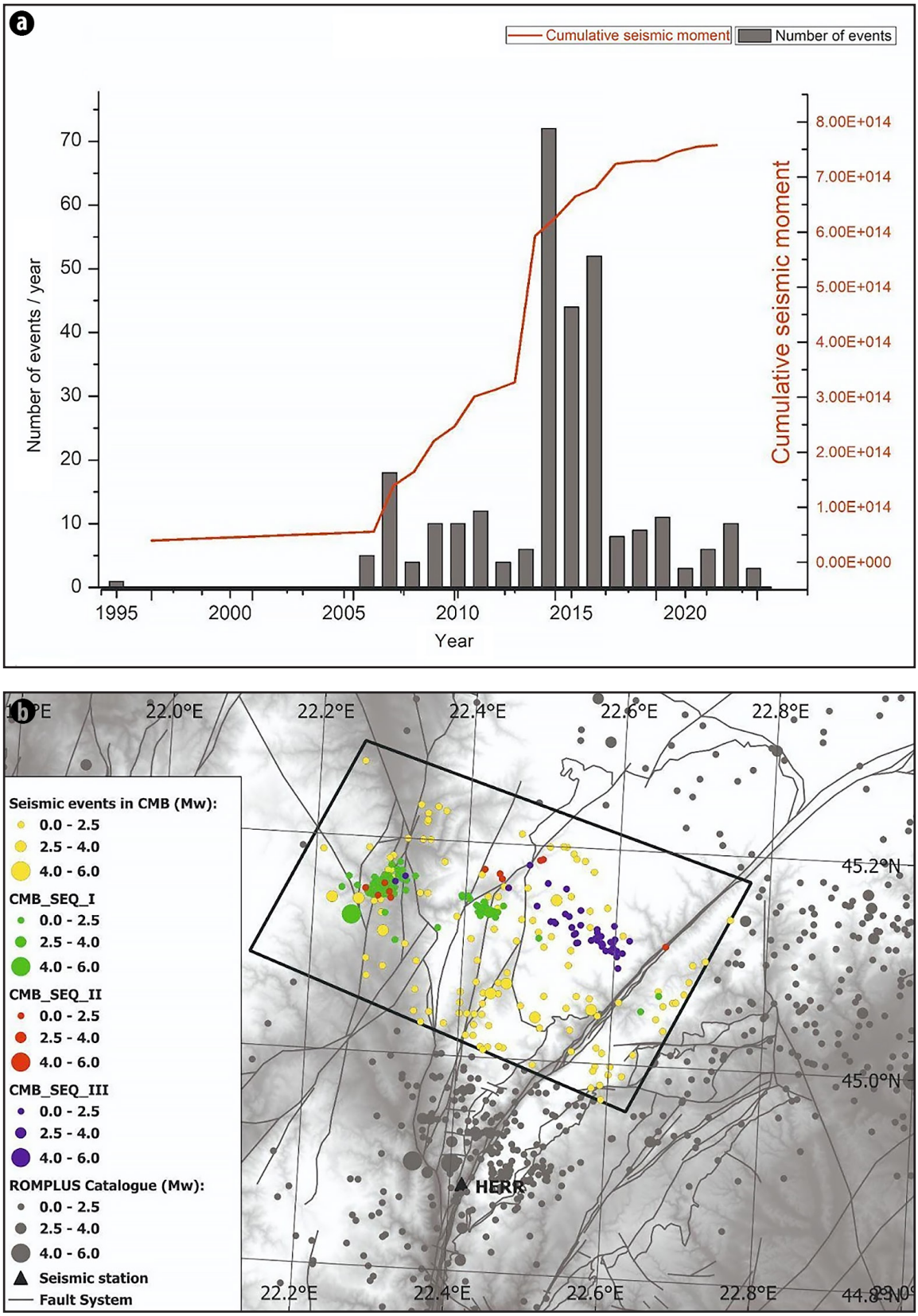

Fig. 4. (**a**) Histogram of the cumulative seismic moment and distribution of the number of events per year, recorded in ROMPLUS between 1995 and 2023 in CMA calculated with the formula: *Mw = (log10M0 – 9.1)/1.5 = (2/3) (log M0 – 9.1)* (IASPEI, 2005; Borman and Giacomo, 2010); (**b**) Spatial distribution of the ROMPLUS events for the CMA between 1995-2023 (yellow colour); Sequences: 1 (green), 2 (red), 3 (blue). The seismic events are Mw-related symbol size.

Cross-correlation analysis is an efficient technique to identify events belonging to a cluster when the distance between hypocentres is sufficiently small (Waldhauser and Ellsworth, 2000).

The cross-correlation coefficient (CC) is a degree of the similarities between pairs of events recorded by the common station and, at the same time, is a measure of the hypocenters proximity in space. We use the cross-correlation technique to identify new events missed by routine seismic analysis. The cross-correlation is used for time windows of 21s on the vertical component recorded by the closest station (HERR) filtered with a Butterworth band-pass filter between 1 and 5 Hz. The template events are selected as representatives for different groups of earthquakes. An earthquake is considered to belong to a cluster if the CC factor is greater or equal to 0.7.

Four template events were selected to cover the epicentral area for the sequences of this study as follows: (**1**) 31/10/2014 – 23:11:18 Mw = 1.9 as part of sequence *Ia*; (**2**) 09/01/2015 – 01:31:52 Mw = 2.6 as part of sequence *Ib*; (**3**) 17/12/2015 – 00:01:29 Mw = 1.8 as part of sequence *II*; (**4**) 30/07/2016 – 08:11:48 Mw = 2.0 as part of sequence *III*. For each template, the entire study interval (31/10/2014 – 31/12/2016) is inspected to detect and locate similar waveforms. Only the pairs of events with a CC greater than 0.7 will be considered as belonging to a specific cluster in our analysis. Examples of correlated waveforms for the first template are plotted in figure 5.

With the first template event and cross-correlation analysis applied, for 2014-2016 time period, were detected 297 events with 0.7≤CC<0.8, 39 events with 0.8≤CC<0.9 and 12 events with 0.9≤CC≤1.0. The high number of correlations with 0.7≤CC<0.8 is explained by potential co-located events (not possible to locate with standard procedures which require acceptable signal-to-noise recordings from a minimum of three stations, so not included in the ROMPLUS).

The template (1) correlates with 44 events from ROMPLUS from sequence I (39 events), sequence II (3 events) and sequence III (2 events). We identify 11 new events (not recorded in the ROMPLUS): 10 events in sequence I and one event in sequence II. These events have local magnitudes (ML) between 0.3 and 1.5 and depths between 1 and 25 km. For them, we found at least three stations with acceptable P and S waves onsets and they were located with routine analysis (Fig. 6b).

The CC analysis for the template (2) led to a group of 34 events: 7 events with 0.7≤CC<0.8, 6 events with 0.8≤CC<0.9 and 21 events with 0.9≤CC<1.0. From these co-located events, 19 events belong to ROMPLUS (18 events with 0.9≤CC<1.0 and 1 event with 0.8≤CC<0.9), 7 are new events (located using at least 3 stations) and 8 events could not be detected by the surrounding stations and could not be located (Fig. 6b).

The CC analysis using the third template (3) resulted in 178 correlated waveforms with 0.7≤CC<0.8; 16 correlated waveforms with 0.8≤CC<0.9 and 7 correlated waveforms with 0.9≤CC<1.0. From these correlated events, only 4 events can be found in the ROMPLUS (0.9≤CC<1.0), 2 events from sequence II and 2 events from sequence III. This large discrepancy between the set of events with CC≥0.7 (as computed using the HERR station) and the events located in ROMPLUS is explained in part by the lack of additional stations with reliable waveforms to allow location.

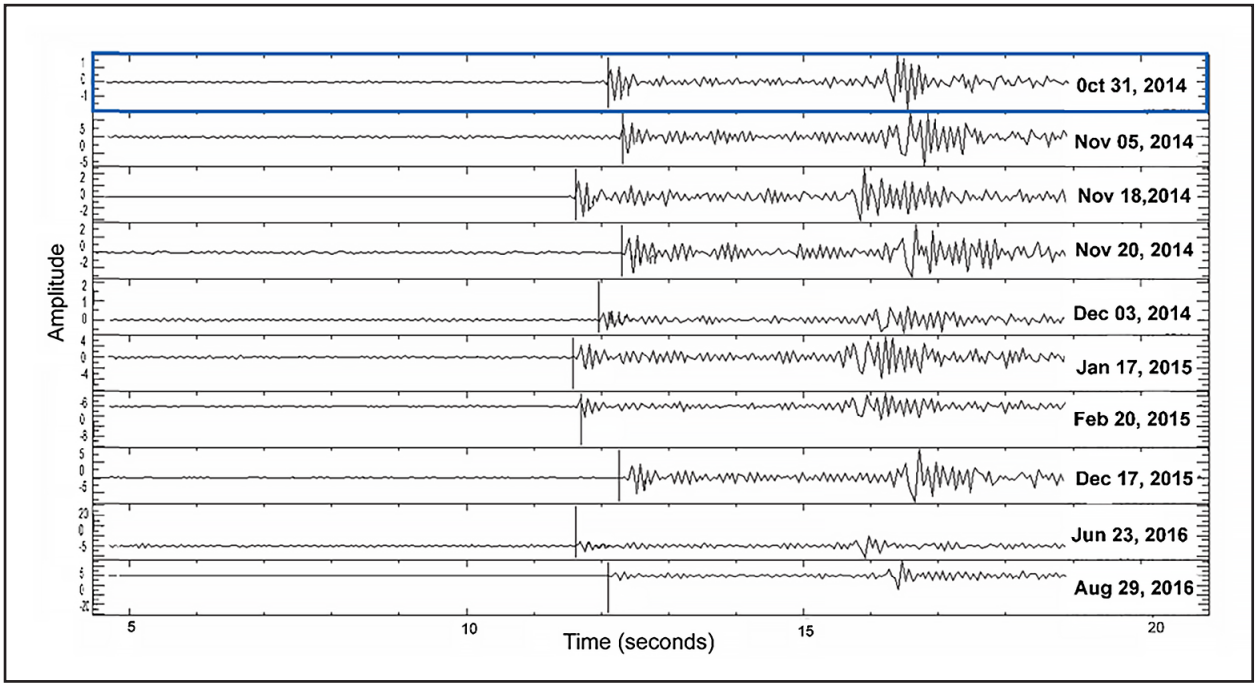

Fig. 5. Waveform display for the template of 31/10/2014 – 23:11:18 (first trace, highlighted in blue) and associated waveforms that correlate with CC factor above 0.9 recorded at HERR (Herculane) station displayed with SAC software. A Butterworth bandpass filter of 1-5 Hz is applied.

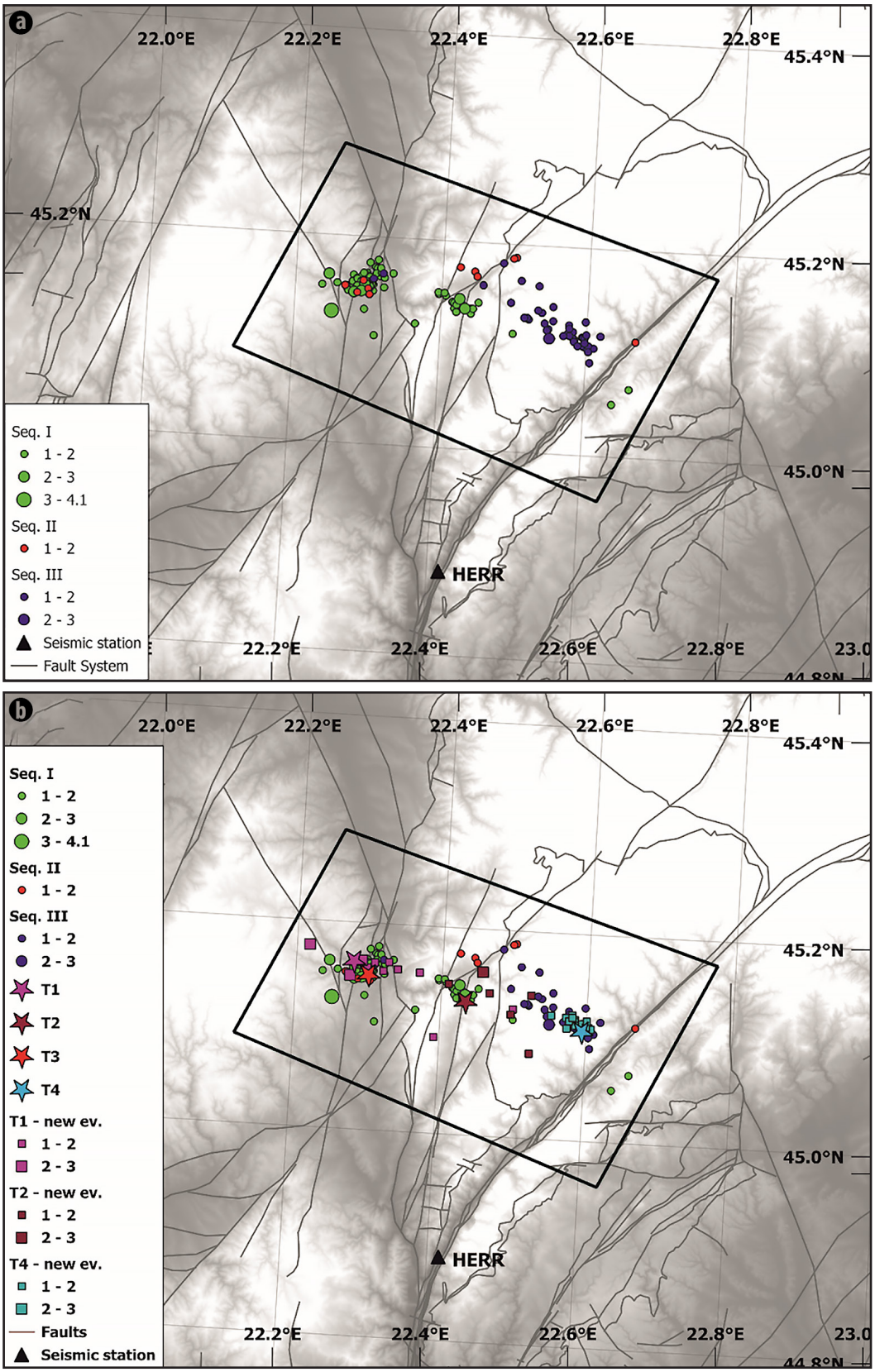

Fig. 6. (**a**) Spatial distribution of the CMA events before cross-correlation where Seq. I – seismic sequence from 31/10/2014 – 05/03/2015; Seq. II – seismic swarm from 23/11/2015 –28/12/2015; Seq. III – seismic swarm from 27/07/2016 – 29/08/2016; (**b**) Spatial distribution of the events from ROMPLUS after cross-correlation, templates T1, T2, T3, T4 (stars) and the new events obtained after cross-correlation with Mw related symbol size (T1 – new events; T2 - new events; T3 - no new events fulfilling the event location criteria; T4 - new events).

The fourth template (4) resulted in 22 correlated waveforms with 0.7≤CC<0.8; 23 correlated waveforms with 0.8≤CC<0.9 and 16 correlated waveforms with 0.9≤CC<1.0. The template (4) correlated with 32 events from ROMPLUS, all events located in sequence III, 6 events with a 0.7≤CC<0.8, 12 events with 0.8≤CC<0.9 and 15 events with 0.9≤CC<1.0. The cross-correlation resulted in 19 new events, 11 with 0.7≤CC<0.8 and 8 with 0.8≤CC<0.9. The new events have local magnitudes (ML) between 0.1 and 0.8 and depths between 1.0 and 14 km. All the new events are part of the sequence III. The number of stations used in localization is between 3 and 6 (Fig. 6b).

6. FOCAL MECHANISMS SOLUTIONS

The fault plane solutions for the studied earthquakes are extracted from two sources: Popa *et al.* (2018) and this work and are represented in figure 1b.

For the largest event from 31/10/2014 the fault plane solutions obtained by different approaches are quite similar to each other with slight variations (within ± 150 for azimuth and ± 50 for plunge) in nodal plane orientation and inclination (Fig. 1c). As shown by previous investigations, it is problematic to decide on the orientation of the rupture plane: Placintă *et al.* (2016) considered the WNW-ESE-oriented nodal plane as rupture plane, while Popa *et al.* (2018) considered the NEN-SWS nodal plane as rupture plane. The first is following the seismicity WNW-ESE alignment; the second is matching the orientation of the main faults in the region (Fig. 1c). The same ambiguity persists for the sequence of 2015.

The fault plane solutions computed in this paper for the 2016 sequence are plotted in figures 7 and 8. We applied the SEISAN software (Havskov and Ottemöller, 2001) to determine the fault plane solutions for 10 events (Table 1). We use both S/P amplitude ratios and P-wave polarities to confine the focal mechanisms. In this case, the solutions are close to a strike-slip faulting with a compression axis oriented in SE-NW direction (Fig. 1c, Fig. 7, Fig. 8). Distribution on depth on two vertical cross-sections and epicentral map outlines the alignment of hypocentres along the WNW-ESE fault for 10 events of the 2016 seismic sequence with fault plane solutions. A careful look at figure 1c shows the presence of a WNW-ESE-oriented local fault fitting well to the alignment of the hypocentres. Orientation of the nodal planes for the 10 events with computed focal mechanism is quite dispersed. The prevalent orientation is ENE-WSW rather than WNW-ESE. This discrepancy between the nodal planes and seismicity directions can be attributed to inherent errors in determining the fault plane solutions.

The Miocene NE translation and clockwise rotation of the Carpathians Orogen with respect to western corner of the Moesian Platform, is well illustrated by NE-SW right-lateral displacements/faults observed throughout the region.

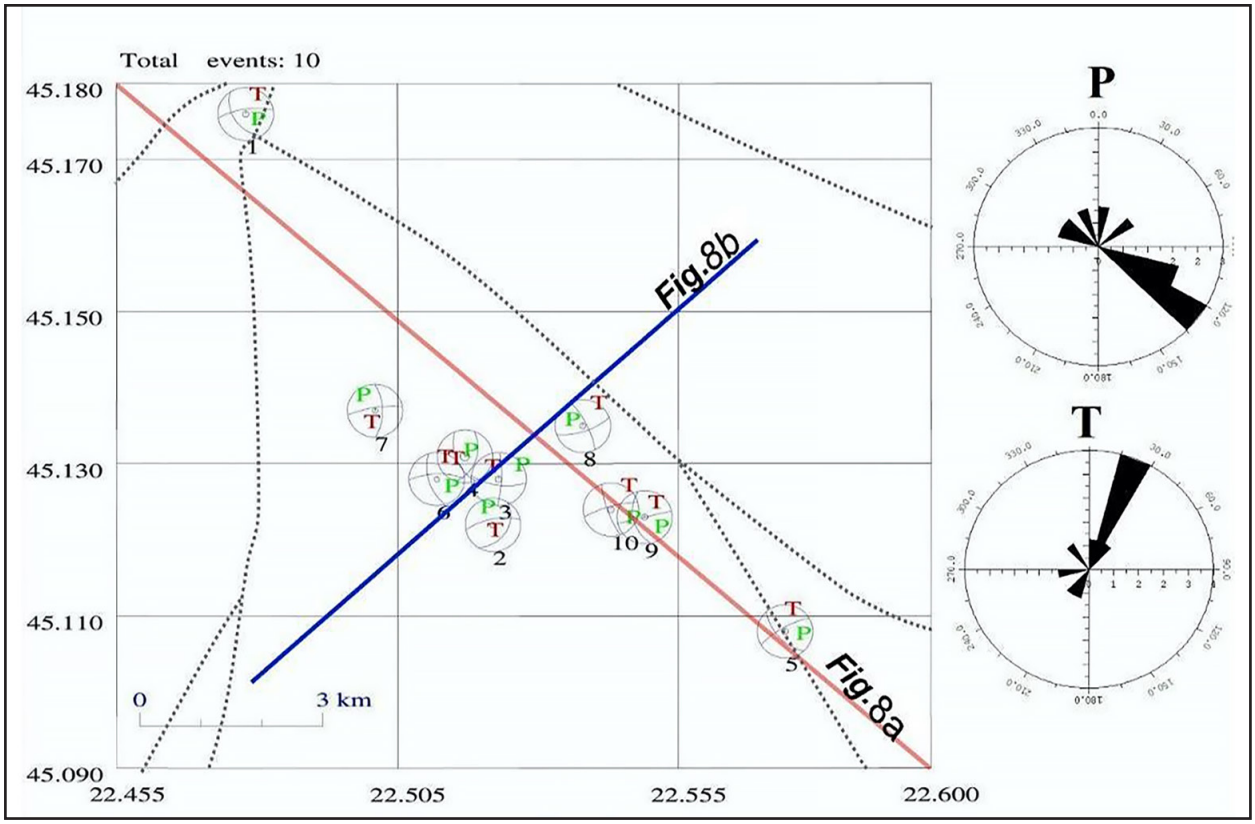

Fig. 7. Epicentral map of 10 events from the 2016 seismic sequence for which the focal mechanism was estimated (left) and azimuthal distribution of the P and T axes (right). The faults in the area are represented with dotted lines.

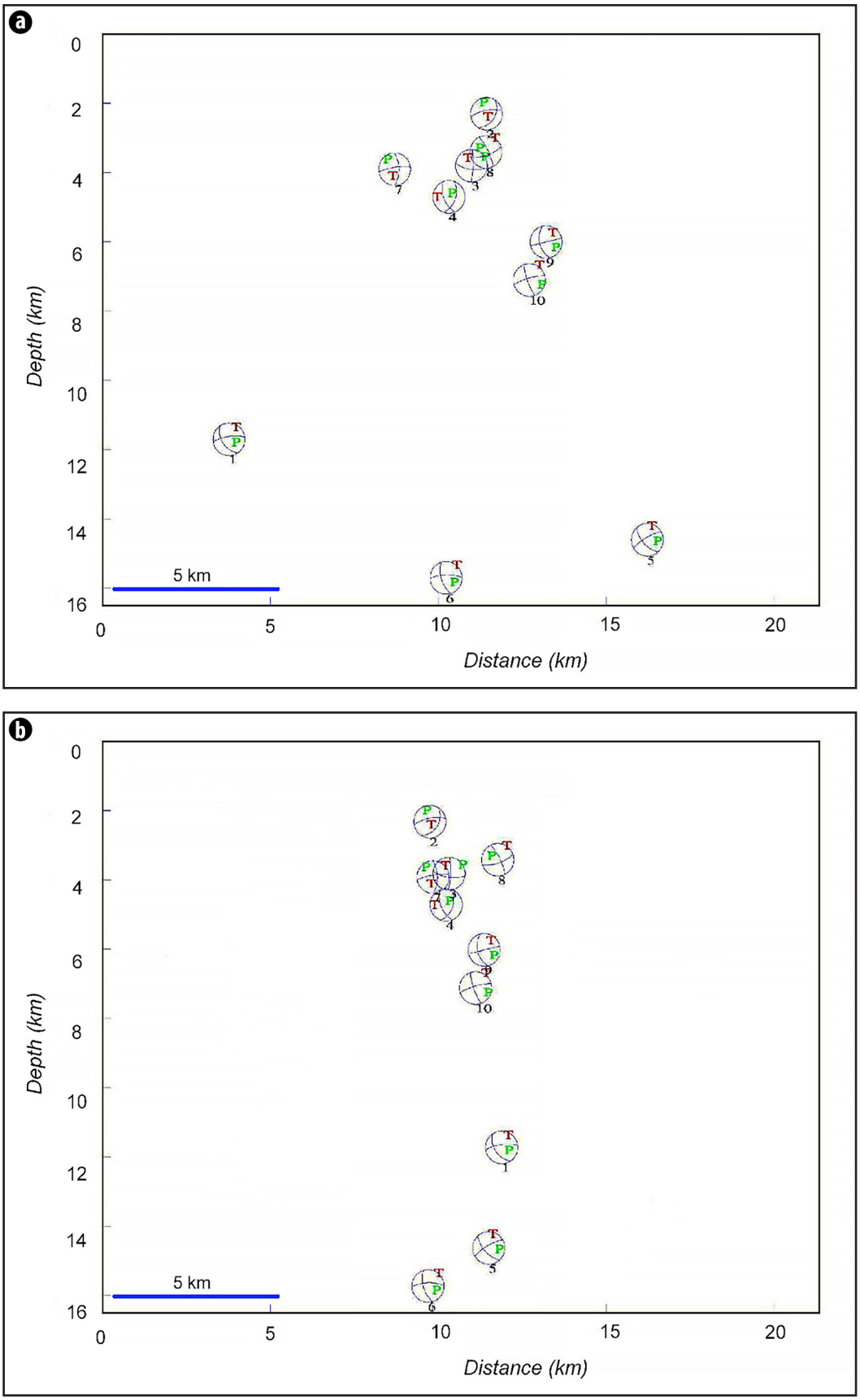

Fig. 8. Hypocentre distribution of the events from the 2016 sequence with fault plane solutions on NW-SE (**a**) and NE-SW (**b**) cross-sections. The distribution of depth on two vertical cross-sections is represented in Fig 2 and outlines the alignment of hypocentres along the WNW-WSE fault.

Table 1. List of the events from the 2016 seismic sequence with focal mechanisms.

Event No.	Year	Month	Day	Hour	Minute	Seconds	Latitude (°N)	Longitude (°E)	Strike	Dip	Rake
1	2016	6	18	19	29	23.2	45.176	22.478	261	69	-127
2	2016	7	30	6	18	7.7	45.13	22.517	259	66	114
3	2016	7	30	8	11	48.2	45.128	22.523	2	78	154
4	2016	7	30	16	5	3.5	45.131	22.517	158	53	-117
5	2016	7	31	4	12	28	45.108	22.574	240	73	-144
6	2016	7	31	15	56	6.2	45.128	22.512	268	68	-143
7	2016	8	1	5	28	12.8	45.137	22.501	261	76	148
8	2016	8	1	7	27	15.5	45.135	22.538	71	66	-161
9	2016	8	1	17	37	1.7	45.123	22.549	77	90	135
10	2016	8	1	17	38	29.6	45.124	22.543	254	76	-164

However, our findings indicate that the apparent alignment and migration of the earthquakes that occurred in the 2014 – 2016-time interval does not correspond to the main trend of the faulting system in the CMA. We interpret our results by assuming a process of successive loadings and releases of deformation migrating in the WNW-ESE direction with right-lateral displacements along an echelon of NE-SW faults in the first stage (2014 – 2015) and then triggering a swarm-type sequence on a local WNW-ESE fault in the second stage (2016).

We encounter a challenge when interpreting the predominant WNW-ESE seismicity configuration with the computed fault plane solutions. To interpret the NE-SW direction of the faulting as indicated by the focal mechanism with the perpendicular direction of the hypocentres migration which characterizes the earthquakes produced first mostly in the western part of the study area, we assumed a step-like process triggering successive ruptures migrating from the West to East, with slip vector lying along parallel NE-SW oriented faults. As the earthquake generation process evolves in space and time, it looks like the slip vector rotates along a local WNW-ESE oriented fault generating in the eastern segment the swarm-type sequence in 2016. Our findings support a complex geotectonic setting with earthquakes produced at the intersections of different fault systems, matching both the dominant NE-SW orientation, parallel to the Carpathians geographical configuration, and secondary faults oriented perpendicularly relative to the main system.

7. DISCUSSION AND CONCLUSIONS

The Carpathian Orogen, Romanian segment, has a double arcuate shape configuration acquired during the Cretaceous-Neogene tectonic processes of northward translation and subsequent eastward rotation of the Dacia mega-unit plate. The two bend zones, the Eastern Carpathian Bend and the Western Carpathian Bend and Danubian seismic region are affected by active seismicity, mainly concentrated in the SECBZ, also known as Vrancea region. The SECBZ is affected by strong earthquakes generated in the mantle range (up to 200 km depth). The SWCBZ is characterized by crustal events, with depths up to 50 km. Although less active than SECBZ, the SWCBZ seismotectonics is important in understanding the tectonic evolution of the Carpathian Orogen. The SWCBZ is affected by neotectonics deformation related to late-stage continental collision processes defining the Carpathian Orogen. The continental collision took place during Late Paleogene-Miocene times, with right lateral rotation of the Carpathian orogen along the western side of the Moesian Platform (Ratschbacher *et al.* 1993; Linzer *et al.* 1998). As a result of this process, a complex structural framework was generated, with main faults direction ranging from NW-SE to NE-SW and intermediate directions that locally produced pull-apart basins with well-defined shapes or pop-up structures such as the BB, in an area dominated by strike-slip related deformation.

The Romanian Seismic Network development in the last decades has contributed to a significant increase of the recorded events and at the same time to the decrease of the threshold magnitude of the earthquakes detected and located in the SWCBZ, in the intra-mountains basins, such as the CMB studied in this paper or at the orogenic contact between the Carpathian Orogen and the Moesian Platform.

Recently (2014 - 2016), the seismic activity in the CMA was characterized by an enhancement through three clusters of events (sequences) consisting of small-to-moderate earthquakes. The activity started on the 31st of October 2014 with a moderate-magnitude earthquake (Mw = 4.1) which triggered in a first stage associated aftershocks and then two other sequences delayed in time and shifted in space.

A WNW to ESE alignment has been activated, with seismicity migrating from west to east. This migration can be explained by the shape of the tectonic contact between the Median and Marginal Dacides which changes its orientation from NNE-SSW to E-W. Seismic release in separate and local-

scale bursts reflects the complex structure of the tectonic faulting of the area.

To better constrain the results, we applied cross-correlation analysis and relocated the earthquake hypocentres after analysing the errors in location and reconsidering the picking of arrival times. We determined the fault plane solutions for all the events for which the solutions can be considered sufficiently well-constrained.

Our approach allowed us to detect a significant number of small-magnitude events belonging to the sequence, in addition to the routine (ROMPLUS) catalogue. Our results for the sequence I (from 31/10/2014 until 05/03/2015) showed that the main shock event was followed by 104 aftershocks. Two other seismic sequences were swarm-type with small magnitudes (Mw < 2.5). In sequence II (from 23/11/2015 until 28/12/2015) occurred 12 seismic events and in sequence III (from 27/07/2016 until 29/08/2016) occurred 61 events.

The epicentral distribution shows clearly a migration from West to East suggesting a possible post-triggering effect after the 2014 sequence.

The analysis of the fault plane solutions for the study sequences is in favour of a predominant NE-SW fault orientation in the first stage (2014 - 2015) in agreement with the prevalent faulting orientation in the region. In the second stage, the strike-slip displacement is moved toward the East and finally rotated to a WNW – ESE direction for the last sequence (2016). The last alignment matches a local fault developed in the same direction. As a general trend, the fault plane solutions indicate an extensional regime with associated normal and strike-slip faulting. Extensional principal axes are oriented mainly in N-S and NE-SW directions, while the compressional principal axes are E-W to SE-NW oriented.

Our results are in favour of a complex geotectonic setting with earthquakes generated at the intersections of different fault systems, one with dominant NE-SW orientation, parallel to the Carpathians geographical configuration, and other local E-W oriented fault systems. The Upper Cretaceous – Paleogene initial fault has been gradually rotated during time to the present-day position creating new fault systems and offsetting the initial system during Miocene-Pliocene times, being currently reactivated in the WNW-ESE compressional regime in case of the CMA as proved by the fault plane solution of the event from 31st of October 2014, the events from 2015 and the events from 2016.

ACKNOWLEDGMENTS

The data processed in this paper are recorded by Romanian Seismic Network and owned by the National Institute for Earth Physics. ROMPLUS catalogue (NIEP). This study has been accomplished through the NUCLEU Programme supported by the Ministry of Research, Innovation and Digitalization, SOL4RISC, PN23360101: "Advanced research for modelling natural and anthropogenic phenomena in the coupled earth-atmosphere system to reduce associated risks".

REFERENCES

Berza, T, Drăgănescu, A. (1988). The Cerna-Jiu fault system (South Carpathians, Romania), a major Tertiary transcurrent lineament". *D.S. Inst. Geol. Geofiz.*, **72-73**: 43-57, București.

Linzer, H.G., Frisch, W., Zweigel, P., Girbacea, R., Hann, H.P., Moser, F. (1998). Kinematic evolution of the Romanian Carpathians. *Tectonoph.,* **297**(*1-4*): 133-156, ISSN 0040-1951, https://doi.org/10.1016/S0040-1951(98)00166-8

Maţenco, L., Bertotti, G., Leever, K., Cloetingh, S., Schmid, S., Tărăpoancă, M., Dinu, C. (2007). Large-scale deformation in a locked collisional boundary: interplay between subsidence and uplift, intraplate stress, and inherited lithospheric structure in the late stage of the SE Carpathians evolution. *Tectonics*, **26**: 1-29, TC4011, doi: 10.1029/2006TC001951.

Maţenco, L., Radivojevic, D. (2012). On the formation and evolution of the Pannonian Basin: Constraints derived from the structure of the junction area between the Carpathians and Dinarides. *Tectonics*, **31** (*6*): 1-31, TC6007, doi: 10.1029/2012TC003206.

Oncescu, M.,C., Mârza, V.I., Rizescu, M., Popa, M. (1999). The Romanian Earthquake Catalogue Between 1984-1997: 43-47, https://doi.org/10.1007/978-94-011-4748-4_4

Oros, E. (2004). The April-August 2002 Moldova Nouă earthquakes sequence and its seismotectonic significance. *Rev. Roum. Geoph*., **48**: 49-68.

Oros, E. (2007(. Macroseismic and instrumental seismicity of the Banat region and its significance on the local seismic hazard and risk. "Thirty years from the Romanian Earthquake of March 4, 1977"; Bucharest, Romania, 1-3 March 2007.

Oros, E. (2011). Cercetări privind hazardul seismic pentru Banat, Ed. Sfântul Nicolae; 393 p. (in Romanian), ISBN: 978-606-30-4261-4.

Oros, E., Diaconescu, M. (2015). Recent Vs. Historical Seismicity Analysis for Banat Seismic Region (Western Part Of Romania). *Math. Model. Civ. Eng.*, **11**(*1*): 1-10, https://doi.org/10.1515/mmce-2015-0001

Oros, E., Popa, M., Moldovan, I.A. (2008). Seismological DataBase for Banat Seismic Region (Romania)-Part 1: The Parametric Earthquake Catalogue. *Rom. J. Phys.,* **53**(*7-8*): 955-964.

Placintă, A., Popescu, E., Borleanu, F., Radulian, M., Popa, M. (2016). Analysis of source properties for the earthquake sequences in the South-Western Carpathians (Romania). *Rom. Rep. Phys.*, **68**(*3*): 1240-1258.

Popa, M., Chircea, A., Dinescu, R., Neagoe, C., Grecu, B., Borleanu, F. (2022). Romanian Earthquake Catalogue (ROMPLUS) 984-2022, Mendeley Data, V2, doi: 10.17632/tdfb4fgghy.

Popa, M., Munteanu, I., Borleanu, F., Oros, E., Radulian, M., Dinu, C. (2018). Active tectonic deformation and associated earthquakes: a case study – South West Carpathians Bend Zone. *Act. Geod. Geoph.,* **53**: 395-413, https://doi.org/10.1007/s40328-018-0224-1

Popescu, E., Radulian, M. (2001). Source characteristics of the seismic sequences in the Eastern Carpathians foredeep region (Romania). *Tectonoph.*, **338**(*3-4*): 325-337.

Radulian, M., Popescu, E., Borleanu, F., Diaconescu, M. (2014). Source parameters of the December 2011 - January 2012 earthquake sequence in Southern Carpathians, Romania. *Tectonoph.*, **623**: 23-38.

Radulian, M., Vaccari, F., Mândrescu, N., Panza, G.F., Moldoveanu, C.L. (2000). Seismic Hazard of Romania: Deterministic Approach. *Pure Appl. Geoph.*, **157**: 221-247.

Ratschbacher, L., Linzer, H.G., Moser, F., Strusievicz, R.O., Bedelean, H., Har, N., Mogoş, P.A. (1993). Cretaceous to Miocene thrusting and wrenching along the central south Carpathians due to a corner effect during collision and orocline formation. *Tectonics*, **12**(*4*): 855-873, doi: 10.1029/93TC00232.

Săndulescu, M. (1984). Geotectonica României, Ed. Tehnică, Bucharest (in Romanian).

Săndulescu, M. (1988). Cenozoic tectonic history of the Carpathians, in The Pannonian Basin. A Study in Basin Evolution. *In*: L.H. Royden and F. Horváth (Eds.), *AAPG Mem.,* **45**: 17-25.

Săndulescu, M., Krautner, H., Borcoş, M., Năstăseanu, S., Patrulius, D., Ştefănescu, M., Ghenea, C., Lupu, M., Savu, H., Bercia, I., Marinescu, F. (1978). Geological map of Romania. *In*: IGR (Ed.). Geology Atlas, sheet no 1., IGR, Bucharest.

Schmid, S., Bernoulli, D., Fügenschuh, B., Maţenco, L., Schefer, S., Schuster, R., Tischler, M., Ustaszewski, K. (2008). The Alpine-Carpathian-Dinaridic orogenic system: correlation and evolution of tectonic units. *Swiss J. Geosci.,* **101**: 139-183.

Ştefănescu, M. and the working group (1988). Geological cross-section at scale 1:200.000, no. B 1-7. Inst. Geol. Geofiz., Bucharest.

Waldhauser, F., Ellsworth, W.L. (2000). A Double-Difference Earthquake Location Algorithm: Method and Application to the Northern Hayward Fault, California. Bull. Seism. Soc. Amer., **90** (6): 1353-1368.

Internet references

ROMPLUS catalogue (http://www.infp.ro/data/romplus.txt).

USGS earthquakes catalogue (https://earthquake.usgs.gov/).